Effects of Mesh Size in a Flat Evaporator and Condenser Cooling Capacity on the Thermal Performance of a Capillary Pumped Loop

Joon Hong Boo*
(*Hankuk Aviation University*)

The thermal performance of a flat evaporator for capillary pumped loop (CPL) applications was investigated. Two to four layers of coarse wire screen wicks were placed onto the heated surface to provide irregular passages for vapor flow. The evaporator and condenser were separated by a distance of 1.2 m and connected by individual liquid and vapor lines. The wall material was copper and the working fluid was ethanol. The experimental facility utilized a combination of capillary and gravitational forces for liquid return, and distribution over the evaporator surface. The tubing used for vapor and liquid lines was 9.35 mm or less in diameter and heat was removed from the condenser by convection of air. A heat flux of up to 4.9×10^4 W/m^2 was applied to a flat evaporator having dimensions of 100 mm by 200 mm, 20 mm thick. The thermal resistance of the system as well as the temperature characteristics of the system was investigated as the evaporator heat flux and the condenser cooling capacity varied. The performance of the evaporator and effect of condenser cooling capacity were analyzed and discussed.

Key Words : Capillary Pumped Loop, Flat Evaporator, Screen Mesh, Condenser, Thermal Resistance, Heat Flux

1. Introduction

Among various two-phase heat transfer devices developed to fulfill the stringent thermal control requirement, CPL is one of the promising alternatives for meeting the demands of both spacecraft and ground-based electronic thermal control systems. The basic operating principle of CPL is similar to conventional heat pipes in that they utilize the phase change of a working fluid to absorb thermal energy and return the liquid from the condenser to the evaporator through utilization of capillary forces. The major difference between a heat pipe and a CPL is that in the latter, the wick structure is isolated from the evaporator, resulting in a reduction in the overall system pressure drop, and hence a higher heat transport capability.

A majority of the recent literature focused on the design parameters and development of various wicking structures (Kroliczec, *et al.* 1984; Ku, 1993; Ku, *et al.*, 1992). Pohner and Antoniuk (1991) presented the results of adding vapor enhancement grooves to CPL evaporators to increase the heat transfer coefficient between the evaporator pump wall and the vapor by as much as a factor of two. This investigation also introduced a condenser design that could collect noncondensible gases. Dickey and Peterson (1994) conducted an experimental and theoretical investigation of a small CPL that used ammonia as a working fluid. While most of the literature dealing with CPL's involve evaporators that had a circular cross-section, Wulz and Embacher

* Corresponding Author,
E-mail : jhboo@mail.hangkong.ac.kr
TEL : +82-2-300-0107 ; **FAX** : +82-2-3158-2191
Department of Aeronautical and Mechanical Engineering, Hankuk Aviation University, 200-1, Hwajun-dong, Deokyang-ku, Koyang-city, Kyonggi-do 412-791, Korea. (Manuscript Received June 9, 1999 ; Revised September 9, 1999)

(1990) presented the results of a combined experimental and theoretical study of CPL's with flat plate type evaporators.

In the typical design of a CPL, a liquid-saturated porous wick material in the evaporator is placed in contact with a grooved heat transfer surface. The vapor produced during the phase change process, is generated primarily at the contact surface between the liquid surface and the groove edge. The grooves provide a vapor passage through which this vapor can flow. In the past, these vapor passages were made either by machining the grooves into the inner surface of the evaporator or by inserting a thin grooved plate into the evaporator. Boo et al. (1995) placed several layers of coarse wire screen wicks onto the heated surface as a substitute for the grooves. This configuration provided an irregular but contiguous passage for vapor flow. The advantage of this concept includes lower manufacturing costs and ease of installation and maintenance. Although use of a mesh wick structure requires proper selection of the mesh size and configuration, this type of flat evaporator geometry may be quite suitable for applications in the cooling of electronic modules or components.

This study is an extension of the previous one for investigation of a CPL performance having a flat evaporator. The emphasis herein was on the effect of changing coarse screen mesh numbers inside the evaporator, and the effect of cooling capacity of condenser on the overall thermal performance of an air-cooled CPL.

2. Experimental Setup and Procedure

The experimental test facility utilized in the current investigation consisted of an evaporator, a condenser, a vapor line, and a liquid line as shown in Fig. 1. The distance between the evaporator and the condenser was 1.2 m and the system was designed to transport up to a maximum thermal load of 1.0 kW. However, due to limitations imposed by the maximum watt density of the heater, the overall thermal energy available at the evaporator was limited to 800 W. The working fluid used in this experiment was ethanol of

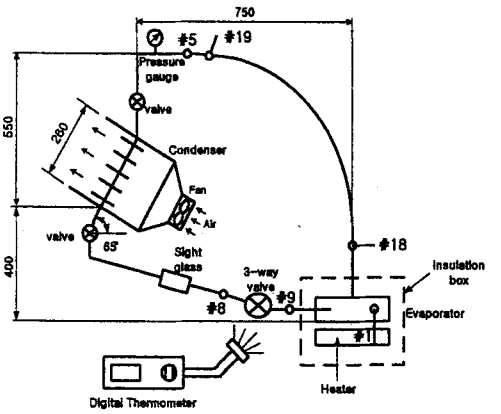

Fig. 1 Schematic of the capillary pumped loop (unit:mm)

99.9±0.2% purity. A flat evaporator, with a dimension of 100 mm×200 mm and 20 mm thick, was fabricated for this study (See Fig. 2). The evaporator consisted of a cover and a container, for easy assembly and to allow changing of the inner screen configuration or cleaning if desired. The cover was fabricated from a 5 mm thick copper plate with five copper tubes 9.53 mm in diameter, silver soldered to the top at five vapor ports (one at the center and one at each of four corners). These copper tubes were joined above the center portion and served as a common vapor header.

The evaporator was made from a solid copper block. The side and the bottom walls were 5 mm thick and a Viton o-ring was inserted between the cover and the container to provide a high vacuum seal. A port for the liquid supply line, a drain port, and a thermocouple compression fittings were provided on the side of the evaporator facing the condenser. The thermocouples were standard grounded T-type probe thermocouples with an uncertainty of 0.5℃ and a diameter of 1.6 mm.

Two to four layers of wire screen were placed on the bottom wall depending on the mesh numbers. On top of the wire screen, a block of ceramic fiber wick, of which the porosity was 0.48 and the dimension was 47 mm×140 mm and 12 mm thick, was placed. The fiber wick block was wrapped with single layer of 100 mesh screen to maintain its shape and to protect the fibers. A grid structure 12 mm high, fabricated from a thin

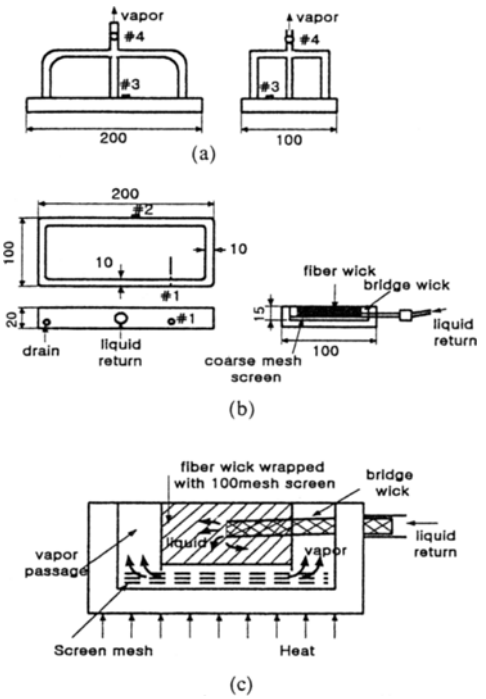

Fig. 2 Schematic of the evaporator (unit : mm)
(a) cover (side and front views)
(b) lower body (side, front, and plane views)
(c) evaporating mechanism in CPL evaporator with wire screen mesh

copper plate was used to hold the screen down firmly onto the bottom surface and to hold the fiber wick in shape. A bridge wick, made by rolling 80 mesh copper screen, was inserted between the liquid inlet port and the fiber wick block to insure the liquid feed to the center of wick block. The vapor evaporated from the bottom of the fiber wick block may escape through pore spaces in coarse mesh screen toward the gap between the sides of block wick and the inner wall of the evaporator, and then to the vapor header above the evaporator cover. This evaporating mechanism is depicted in Fig. 2 (c).

A plate heater was placed underneath the evaporator. The heater unit was 5 mm thick and had the same bottom area as the evaporator. A silicon heat sink compound was applied between the evaporator bottom and the heater surfaces, and a ceramic plate and insulation material were placed under the heater to reduce convective losses. The evaporator and the heater were fastened together by two clamps and placed in a plywood box with a thermal blanket and glass wool inserted in the gap. The heater power was 800 W at a maximum power of 220 V and controlled manually by a variac. The actual heater power was monitored during the experiment using a wattmeter with an experimental uncertainty of 1%.

The condenser was designed as a cross-flow heat exchanger where the hot vapor flow condensed through three finned tubes from top to bottom with 65° slope from the horizontal. The outer diameter of a condenser tube was 12.5 mm and the length of the finned section was 170 mm with fin pitch of 5 mm. The tubes were placed to face the cooling air in parallel and the two side tubes were made to cut off the flow depending on the thermal load. The cooling air was driven by a small fan of 120 mm tip diameter, 30 mm blade length, and 28 W power consumption. The outer wall of condenser was made of transparent acrylic plastic. The volumetric flow rate of the coolant was measured using a pitot-static tube by traversing the cross section. Air temperatures were measured at one point for inlet and at three points at the exit by sheathed thermocouples. The cooling air flow rate and temperatures were used to check the energy balance between the evaporator and condenser. A sight glass was installed at the working fluid outlet of the condenser to confirm the state of the condensate. The outer diameter of the tubing was 9.53 mm except the liquid return line after the 3-way valve, where 6.35 mm o. d. tube was used. High vacuum fittings and valves were employed for tubing. Temperatures were measured using mostly AWG 30 gage K-type thermocouples having uncertainty of 1℃, except four locations measuring vapor temperature, where AWG 30 gage T-type thermocouples probes having uncertainty of 0.5℃ penetrated to the center of the tube. Altogether twenty thermocouples were installed in the system and connected to a data acquisition system. The thermocouple numbers and their locations are shown in Figs. 1 through 3.

The system was carefully cleaned and purged before initial assembly. Prior to charging, a vac-

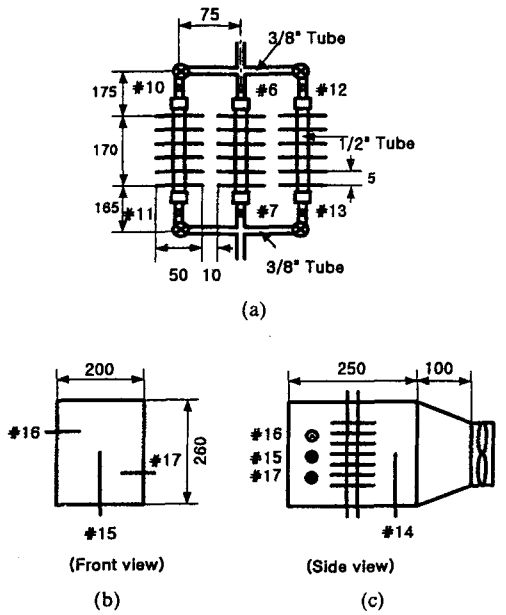

Fig. 3 Schematic of the condenser (unit: mm)
(a) tubes (b) air channel (front view)
(c) air channel (side view)

uum pressure of 0.01 millitorr was achieved at an elevated temperature over 80°C, using a diffusion pump. The liquid charge amount was calculated so that the liquid can fill the whole porous space in fiber wick block and the wire screen mesh, and a part of the liquid return line (6.35 mm o. d. region after the 3-way valve in Fig. 1), before startup. The evaporator was heated before liquid filling for smooth startup of the loop, and to prevent an oscillating liquid column or unstable two-phase movement.

In most conventional CPL's, an auxiliary liquid pump or a dedicated liquid return mechanism is normally employed for reliable operation, especially those used in microgravity environments in spacecraft. However, the liquid return mechanism was simplified in this study to utilize gravity since the evaporator performance was the issue of primary concern.

At a predetermined heater power, real time displays of the temperature were monitored for a minimum of thirty minutes for each 50 W change in heat input. For the analysis of thermal performance, a steady-state temperature distribution was obtained for each test case.

3. Results and Discussion

The thermal performance of the CPL was investigated with three different screen wick configurations located in the flat evaporator. Prior to these tests, the evaporator was first tested without any capillary structure inside to provide baseline performance of the loop. The experiment was conducted with copper screen wicks and heater powers between 25 W and 700 W depending on the cases.

For a specific mesh configuration and a thermal load, the condenser configuration was also varied to identify the effect of the cooling capacity on the system performance. To the possible extent, experiments were conducted with one, two or three condenser passes open and the results were compared with each other.

As a performance index, the thermal resistance of the system can be defined as

$$R_{th}=\Delta T_{sys}/q \qquad (1)$$

where q is the heat transfer rate and ΔT_{sys} is the difference between the evaporator wall temperature and the condenser inlet coolant temperature. Therefore, R_{th} accounts for the overall thermal resistance between the heat source and the heat sink. Typically the thermal resistance is expressed as a function of the heat input.

Figure 4 summarizes the experimental results for the bare evaporator plate by comparing temperatures at five typical points in the system. The practical working mode of these cases was a thermosyphon loop. The liquid charge percent was based on the evaporator internal volume, 216 cc. Figures 4.(a), (c) and (d) show the results for 20% liquid charge case with one, two and three condenser passes open, respectively. Figure 4 (b) shows the typical result for 30% liquid charge with three condenser tubes open. T_{eva}, T_{ci}, T_{co}, T_{ai}, and T_{ao} denote the temperatures at the evaporator wall, condenser inlet, condenser exit, air inlet, and air exit, respectively.

For 10% liquid charge, the evaporator temperature exhibited overheating trend beyond 150 W thermal load. The thermal transport capability of

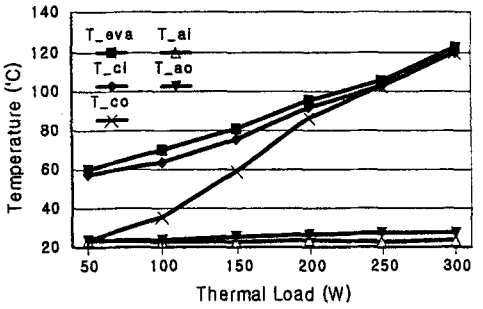

(a)

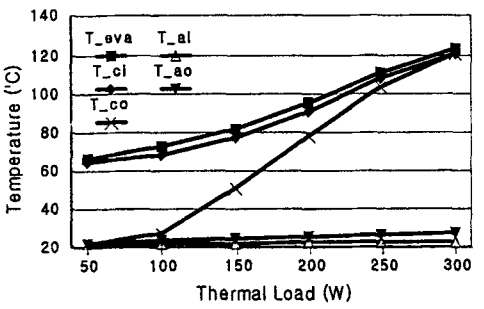

(b)

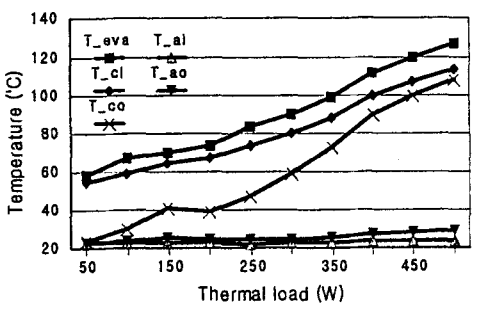

(c)

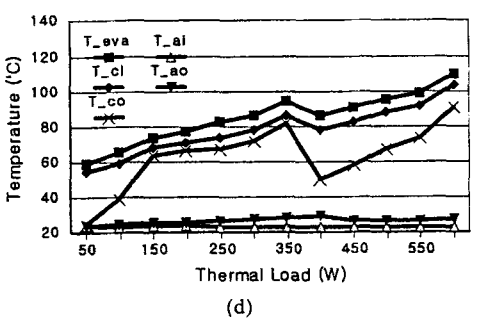

(d)

Fig. 4 System temperature variations with thermal load for bare evaporator plate cases.
(a) 20% charge(1 condenser open) (b) 30% charge(1 condenser open) (c) 20% charge (2 condensers open) (d) 20% charge(3 condensers open)

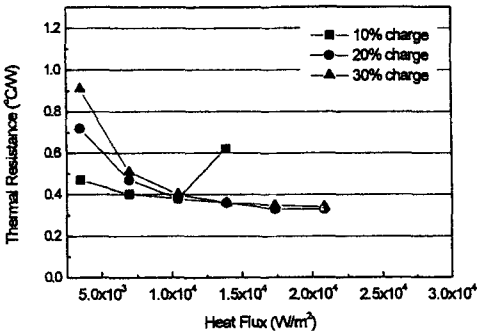

(a)

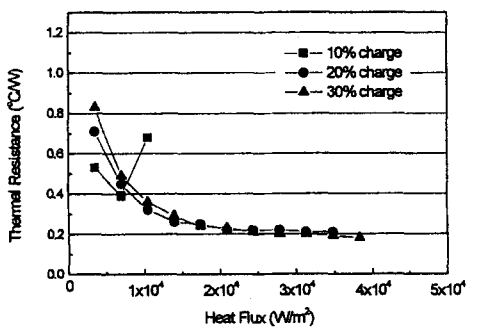

(b)

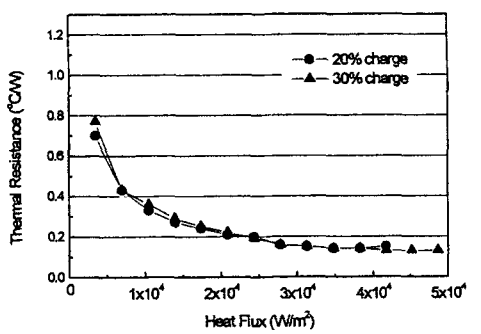

(c)

Fig. 5 Thermal resistance of the system with bare evaporator plate.
(a) one condenser open, (b) two condensers open, (c) three condensers open

the system was enhanced by filling more working fluid. For 20% liquid charge, (a), the maximum temperature in the evaporator was 122℃, which was reduced by 23℃ from 143℃ for 10% liquid charge. To compare (a) and (b), the maximum and minimum temperatures ranged between similar values. However, T_{∞} approached T_{ci} at 200 W in (a) and at 250 W in (b). This point was

considered as a balanced state between the condenser cooling performance and the thermal transport capability of the system. The difference between T_{ci} and T_{∞} is subcooling amount through the condenser. In the case of liquid charge 30% (b), there was subcooling of working fluid in the condenser until the thermal load reached 250 W, while the subcooling ceased and balanced heat transport occurred in the condenser at 200 W for 20% charge case (a).

For 20% liquid charge with two condenser tubes open, (c), the overall temperature range appeared similar to each other and to the cases with one condenser tube open. The major difference was in the temperature at the condenser exit. Enhanced subcooling through the condenser was observed than in the previous cases. This may have been due to the improved cooling capacity of the condenser. Figure 4(d) summarizes the system temperatures with three condenser tubes open, for 20% liquid charge. The maximum temperature in the evaporator has decreased by 15℃ from the cases with two condensers open.

The thermal resistance of the system calculated from the data for bare evaporator plate are summarized in (a), (b) and (c) in Fig. 5 for one, two, and three condensers open cases, respectively. It is obvious that the thermal resistance exhibits exponential decrease with heat flux. At the same thermal load, thermal resistance is decreased as the condenser performance was enhanced. As the number of condenser tubes increased from two to three for example, the relative decrease of the system thermal resistance was about 6% at low heat flux value of 3,500 W/m^2, and the decrease was more than 25% for higher heat flux values around 35,000 W/m^2 or higher. With the same configuration in the condenser, thermal resistance for the lower heat flux range in the evaporator exhibited significant difference depending on the liquid charge. The higher thermal resistance was due to the thicker liquid layer in the evaporator along the heat transfer path. In one condenser tube case, (a) for example, the difference was as much as 0.24℃/W at heat flux of 3,500 W/m^2. However, this difference diminished as the condenser cooling performance was

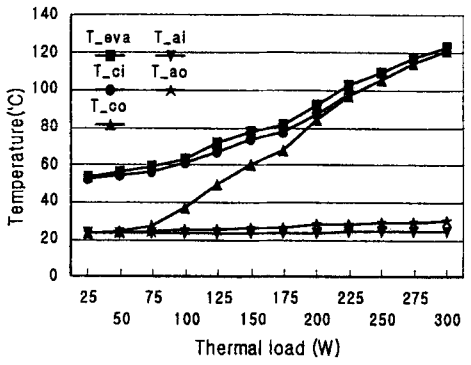

(a)

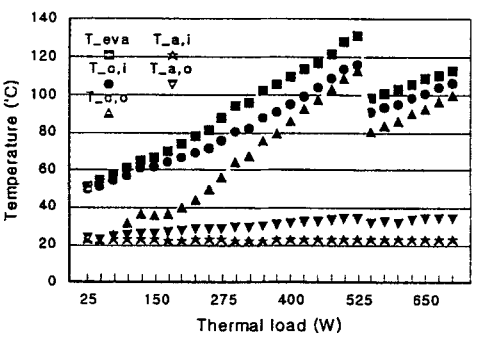

(b)

Fig. 6 System temperature variation with heat flux for two layers of 10 mesh screen.
(a) one condenser tube open,
(b) two and three condensers open

enhanced. The bounced points in (a) and (b) for 10% liquid charge represent unstable state due to dryout trend for underfill. Figure 6 shows system temperature variations with thermal load when 2 layers of 10 mesh wire screen covered the evaporator surface. The liquid charge was 117.6 cc for this configuration. Figure 6 (a) represents the case with one condenser tube open. In Fig. 6 (b), data points for thermal load lower than 550W were for the case with two condenser tubes open, and the rest were with three condenser tubes open. At the same thermal load value, the temperatures were much lower for more condenser tubes open. With one condenser tube open, subcooling in the condenser ceased at 200 W and the evaporator temperature reached 120℃ at 300 W thermal load. As more number of condensers were open, the system temperatures decreased significantly at the same heat load value. For the case with two

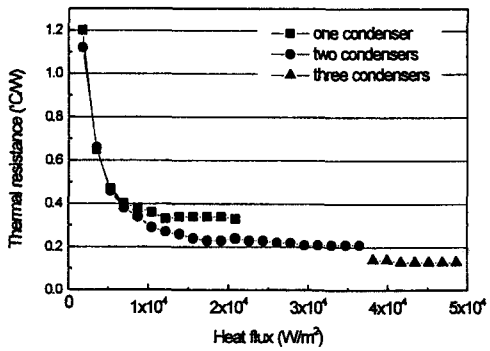

Fig. 7 Thermal resistance of the system with 2 layers of 10 mesh screen and liquid charge of 117.6 cc

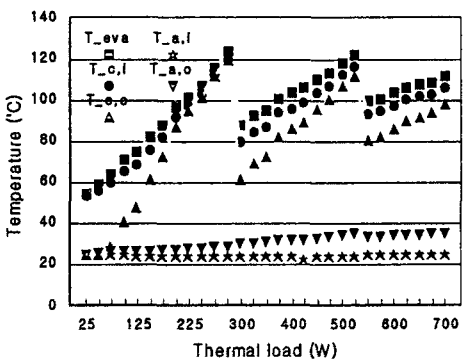

Fig. 8 System temperature variation with thermal load for four layers of 24 mesh screen

condensers open, at 300 W thermal load for example, the evaporator temperature was 26℃ lower and the condenser exit temperature was 58℃ lower than those with one condenser open. These values correspond to 21.7% and 48. 3% relative decrease. While the evaporator temperature increased linearly with thermal load and reached 130℃ at 525 W when two condensers were open, the maximum temperature of the system reached 114℃ at 700 W when three condenser tubes were open. The subcooling in the condenser for three tubes were open was 12℃ at 550 W but reduced to 7℃ at 700 W.

Figure 7 denotes thermal resistance variation with heat flux values. The thermal resistance decreased drastically to about one third of the value until heat flux value of 5,000 W/m², but the difference in thermal resistance among three cases was not appreciable up to this heat flux. However,

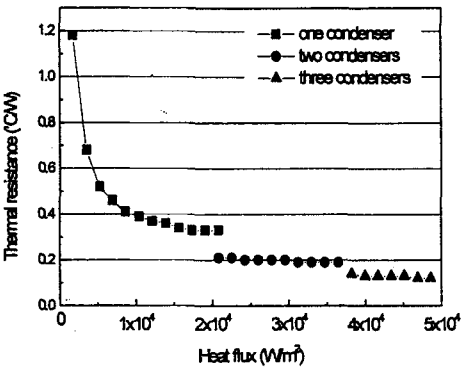

Fig. 9 Thermal resistance of the system with four layers of 24 mesh screen and liquid charge of 119.5 cc

the difference in thermal resistance was distinct (0.1℃/W) among three cases of heat fluxes higher than 20,000 W/m².

Figure 8 summarizes the results when four layers of 24 mesh wire screen covered the evaporator bottom surface. The liquid charge was 119.5 cc for this case. No comparison was made among three cases at the same thermal load. The points for thermal loads lower than 300W were with one condenser tube open, those between 300 W and 525 W were with two condensers open, and the rest were with three condensers open. A change was noticeable in the rate at which the temperatures increased with heat flux. The rate (slope in the figure) was the highest in the case with single condenser tube open, and the lowest in the case with three condenser tubes open. The evaporator temperature increased by only 12℃ as the heat input was increased from 550 W to 700 W. The subcooling rate in the condenser was increased with the number of open condenser tubes. Thermal resistance variation with the heat flux was shown in Fig. 9. Between the cases with one and two condensers open, the difference was 0.12℃/W and that it was 0.06℃/W for heat flux values higher than 40,000 W/m².

Figures 10 and 11 show the results when 3 layers of 60 mesh screen covered the heated plate in the evaporator. The amount of liquid charge was 117.4cc. In Fig. 10, data points between 270W and 525W were for the case with two condenser tubes open. The data in lower thermal

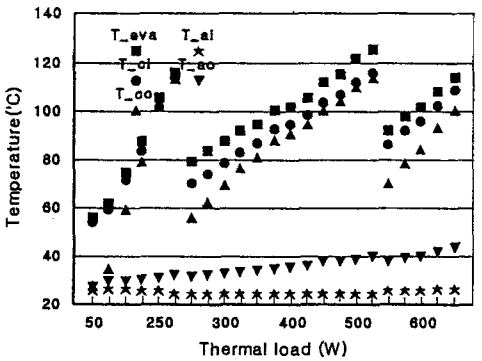

Fig. 10 System temperature variation with thermal load for three layers of 60 mesh screen

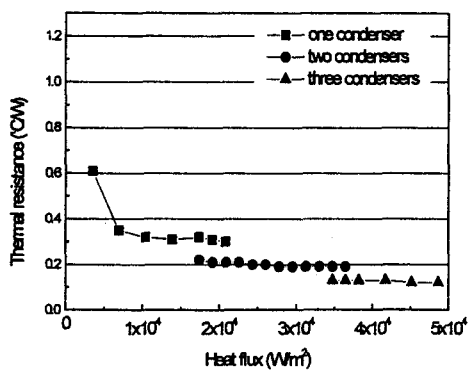

Fig. 11 Thermal resistance of the system with three layers of 60 mesh screen and liquid charge of 117.4 cc

load values were for one condenser tube open, and those in higher thermal load values were for three condenser tubes open. The general trends in temperature were similar to the previous cases, except that T_{∞} approached T_{ci} at lower thermal loads. In Figure 11, lower thermal resistance values were observed than the previous cases with 10 and 24 meshes for heat flux values lower than 1.5×10^4 W/m². The difference was as much as 0.08℃/W. The effect of condenser area increase was similar to other cases with 10 and 24 mesh numbers.

4. Conclusions

In an effort to determine how various screen wick structures in the CPL evaporator affect the system performance, three different coarse wire mesh screens were evaluated up to powers of 700 W with an evaporator footprint area of 0.0144m². These thermal performances were compared with the bare evaporator case. Furthermore, the effect of condenser cooling capacity change was investigated.

The thermal resistance of the system with a screen wick covered evaporator surface ranged from 1.2℃/W at 25 W (heat flux of 1,736 W/m²) to 0.08℃/W at 700 W (heat flux of 48,600 W/m²). With respect to the system thermal resistance as a function of the evaporator heat flux, only minor difference was observed between the screen mesh numbers incorporated, 10, 24, and 60 mesh. This may have been due to the fact that the thermal resistance in the condenser was dominant, which was intrinsic to air-cooled systems, and the change of thermal resistance in the evaporator had only little effect on the overall thermal resistance of the CPL.

The nominal evaporating surface area was larger in the bare plate case than those for screen wick covered evaporator. The fact that the screen wick covered CPL evaporator exhibited almost same thermal performance with the bare plate evaporator implied that the former configuration did work properly. The results also implied that a sufficient evaporating area as well as vapor passage was provided through the pore space between the screen mesh on the evaporator plate and the block wick on top of the screen.

For a configuration with specific mesh numbers, thermal resistance exhibited appreciable difference with the condenser cooling capacity. For heat flux values higher than 20,000 W/m², the difference was about 0.1℃/W between one and two condenser tube configurations, and was 0.08℃/W between two and three condenser tube configurations. The effect of condenser performance was more significant than the mesh numbers inside the evaporator of an air-cooled CPL.

Acknowledgement

The author wishes to acknowledge the financial support of the Korea Research Foundation granted in the program year of 1997 (KRF 1997-001-E00015).

References

Boo, J. H. and Peterson. G. P., 1995, "Experimental Study on the Thermal Performance of a Capillary Pumped Loop Having a Flat Evaporator," Paper No. AIAA-95-3514, Presented at the *ASME/AIAA National Heat Transfer Conference*, August 6-9, 1995, Portland, Oregon.

Dickey, J. T. and Peterson, G. P., 1994, "Experimental and Analytical Investigation of a Capillary Pumped Loop," *Journal of Thermophysics and Heat Transfer*, Vol. 8, No. 3, pp. 602~607.

Kroliczek, E. J., Ku, J. and Ollendorf, S., 1984, "Design, Development and Test of a Capillary Pump Loop Heat Pipe," *AIAA 19th Thermophysics Conference*, June 24-28, Snowmass, Colorado.

Ku, J., 1993, "Overview of Capillary Pumped Loop Technology," ASME HTD, Vol. 236, *Heat Pipe and Capillary Pumped Loops*, pp. 1~17.

Ku, J., Yun, S., and Kroliczek, E., 1992, "A Prototype Heat Pipe Heat Exchanger for Capillary Pumped Loop Flight Experiment," AIAA 92-2910, *AIAA 27th Thermophysics Conference*, July 6-8, Nashville, Tennessee.

Pohner, J. and Antoniuk, D., 1991, "Recent Enhancements to Capillary Pumped Loop Systems," AIAA-91-1375, *AIAA 26th Thermophysics Conference*, June 24-26, Honolulu, Hawaii.

Wulz, H. and Embacher, E., 1990, "Capillary Pumped Loops for Space Applications Experimental and Theoretical Studies on the Performance of Capillary Evaporator Designs," AIAA 90-1739, *AIAA/ASME 5th Joint Thermophysics and Heat Transfer Conference*, June 18-20, Seattle, Washington.